Modeling and simulation of a solar absorption refrigeration machine operating with lithium chloride water coupled (H_2O-LiCl)

Modélisation et simulation d'une machine frigorifique à absorption solaire fonctionnant avec le couple (H_2O-LiCl)

Yosra Ounis, Abdelmajid Saoud, Yasmina Boukhchana, Ali Fellah

Laboratory of Applied Thermodynamic, National Engineering School, University of Gabes, Tunisia,
ounisyosra7@gmail.com, abdelmajidsaoud17@gmail.com, boukchana.yasmina@gmail.com, al.fellah@gmail.com

ABSTRACT. This document presents a thermodynamic analysis of a solar driven single effect lithium Chloride-water (H_2O-LiCl) absorption cooling system. A flat plate collector (FPC) is used to absorb the solar radiation and serve as a source of heat necessary for the operation of the cycle. An energy and exergy-based analysis was carried out for every component of the system. This system is analyzed in respect with a broad range of performance indicators including the coefficient of performance (COP), the cooling capacity (Q_{evap}), total and exergetic effeciency. Under steady state working conditions, the thermal and the mathematical calculation of the single effect chiller at each state point and the solar collector performance was simulated using EES tool. The final result shows that the solar absorption installation overall performance is dependent on various number of parameters (T_{GEN}, T_{ABS}, T_{COND}, T_{EVAP}). According to a parametric study it was found that the generator and evaporator temperature improves the cooling capacity and the coefficient of performance of chiller which is not the case for absorber and condenser temperatures. Furthermore, the exergy destruction is maximum at both the generator and absorber while it is less at the evaporator and condenser and approximately null at expansions valves and solution pump.

RÉSUMÉ. Ce document présente une analyse thermodynamique d'un système de refroidissement par absorption simple effet à base de chlorure de lithium et d'eau (H_2O-LiCl). Un collecteur plat (FPC) est utilisé pour absorber le rayonnement solaire et servir de source de chaleur nécessaire au fonctionnement du cycle. Une analyse énergétique et exergétique a été réalisée pour chaque composant du système. Ce système est analysé en fonction d'une large gamme d'indicateurs de performance, notamment le coefficient de performance (COP), la capacité de refroidissement (Qevap), l'efficacité totale et l'efficacité énergétique. Dans des conditions de fonctionnement en régime permanent, le calcul thermique et mathématique du refroidisseur à simple effet à chaque point d'état et la performance des capteurs solaires ont été simulés à l'aide de l'outil EES. Le résultat final montre que la performance globale de l'installation d'absorption solaire dépend d'un certain nombre de paramètres (T_{GEN}, T_{ABS}, T_{COND}, T_{EVAP}). Selon une étude paramétrique, il a été constaté que la température du générateur et de l'évaporateur améliore la capacité de refroidissement et le coefficient de performance du refroidisseur, ce qui n'est pas le cas pour les températures de l'absorbeur et du condenseur. En outre, la destruction d'énergie est maximale au niveau du générateur et de l'absorbeur, alors qu'elle est moindre au niveau de l'évaporateur et du condenseur et à peu près nulle au niveau des vannes d'expansion et de la pompe de solution.

KEYWORDS. Absorption cooling chiller, Exergetic efficiency, Energetic analysis, Coefficient of performance, Lithium Chloride-water.

MOTS-CLÉS. Réfrigérateur à absorption, Efficacité énergétique, Analyse énergétique, Coefficient de performance, Chlorure de lithium-eau.

1. Introduction

Many alternative energy sources can be used instead of fossil fuels. The decision as to what type of energy source should be utilized in each case must be made on the basis of economic, environmental, and safety considerations. Because of the desirable environmental and safety aspects it is widely believed that solar energy should be utilized instead of other alternative energy forms because it can be provided sustainably without harming the environment [1].

If the world economy expands to meet the expectations of countries around the globe, energy demand is likely to increase, even if laborious efforts are made to increase the energy use efficiency. It is now generally believed that renewable energy technologies can meet much of the growing demand at prices that are equal to or lower than those usually forecast for conventional energy[2]. For this reason, absorption refrigeration systems driven by solar energy are receiving significant research interest in the recent years. Furthermore, the ARS typically uses water as a refrigerant and the working fluids of system operation are environmentally friendly with zero global warming potential (GWP) and ozone depletion potential (ODP). In the ARS, the type of absorbent–refrigerant pair selected plays a major role in performance. Among them, the most commonly used pairs are lithium bromide-water (LiBr-H_2O), lithium chloride-water (LiCl-H_2O) for a higher coefficient of performance (COP) and aqua ammonia (H_2O-NH_3) for producing cold at a lower temperature level[3].

This paper presents the energetic and exergetic analysis of solar driven single-effect lithium chloride-water (LiCl-H2O) absorption system. Integration of solar energy system (solar collector) with the absorption chiller was done. The energy and exergy analysis was carried out for each component of the system. Exergy destructions that occurred in each component of absorption chiller system were analyzed. The coefficient of performance and the exergetic efficiency of the system were also analyzed.

2. System description

The single-effect lithium chloride-water (H_2O-LiCl) absorption cooling system consists of the generator, condenser, evaporator, absorber, solution pump (SP), two expansion valves and solution heat exchanger(figure 1). Plat flat collector is used to absorb radiation and serve as a source of heat necessary for the operation of the cycle. It uses water as refrigerant and LiCl solution as absorbent. The schematic diagram of this system is shown in fig 1. The high temperature heat source (11–12) adds heat in the generator to separate water vapor from the weak solution (3). Then, the refrigerant vapor (7) from the generator is condensed by the cooling water (stream 15–16) in the condenser. Afterwards, the liquid refrigerant (stream 8) flows through an expansion valve (EV2) to the evaporator and vaporizes at the saturation temperature to absorb heat from the chilled water (stream 17–18). Subsequently, the refrigerant vapor (10) is conducted to the absorber, where it is absorbed by the strong solution (stream 6) going through the solution expansion valve (EV1) and the whole process is cooled down by cooling water (13–14). Finally, the low concentration solution at the outlet of the absorber (1) is pumped to the generator via a solution heat exchanger (SHE). The pressurized solution (2) is preheated in the SHE by the high-temperature strong solution (4–5) coming from the generator.

3. Mathematical Modeling

3.1. *Absorption cooling system*

3.1.1. *Assumptions*

To simplify the theoretical analysis, some assumptions were made as follow:

- The system runs at steady state for each component of the system
- The refrigerant at the outlet of the condenser and evaporator are saturated liquid and saturated vapor respectively.
- the work of the pump is negligible $Wp \simeq 0$
- the reference system was taken at 25 ◦C and 1 atmospheric pressure.
- Chemical exergy of materials , as well as the kinetic, potential energy and exergy, are neglected as they are relatively very small

- The expansion valves are considered isenthalpic.

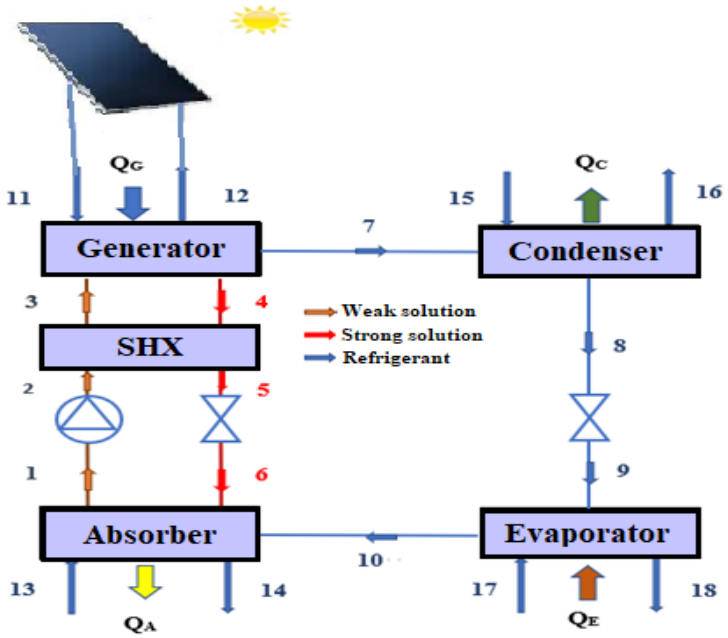

Figure 1. *Schematic of lithium chloride-water absorption cooling system.*

3.1.2. *Thermodynamic formulations*

Inlet and outlet temperatures of cooling or heating streams are presented in table 1

Absorber	***outlet temperature of cooling water (◦C)**	***$T_{14}=T_{abs}-3$**
	***Inlet temperature of cooling water (◦C)**	***$T_{13}=T_{14}-5$**
Evaporator	***Inlet temperature of chilled water (◦C)**	***$T_{17}=T_{evap}+7$**
	***Outlet temperature of chilled water (◦C)**	***$T_{18}=T_{17}-5$**
Condenser	***Outlet temperature of cooling water (◦C)**	***$T_{16}=T_{cond}-3$**
	***Inlet temperature of cooling water (◦C)**	***$T_{15}=T_{16}-5$**
Generator	***Outlet temperature of hot water (◦C)**	***$T_{12}=T_{gen}+3$**
	***Inlet temperature of hot water (◦C)**	***$T_{11}=T_{12}+7$**

Tableau 1. *Inlet and outlet temperatures*

The thermodynamics analysis of the absorption refrigeration system is the process of applying the principles of first and second law of thermodynamics and mass conservation at each component of systems[4]:

Mass balance: $\sum \dot{m}_{in} x_{in} = \sum \dot{m}_{out} x_{out}$

Energy balance: $\sum_{out} \dot{m} . h - \sum_{in} \dot{m} . h = \dot{W} + \dot{Q}$

The energy balances the component in the system are as follows :

$$Q_{ABS} = \dot{m}_6.h_6 + \dot{m}_{10}.h_{10} - \dot{m}_1.h_1$$

$$Q_{GEN} = \dot{m}_4.h_4 + \dot{m}_7.h_7 - \dot{m}_3.h_3$$

$$Q_{COND} = \dot{m}_7.h_7 - \dot{m}_8.h_8$$

$$Q_{EVAP} = \dot{m}_{10}.h_{10} - \dot{m}_9.h_9$$

$$\dot{Q}_{EDC} = \dot{m}_4.h_4 - \dot{m}_5.h_5$$

$$\dot{Q}_{EDC} = \dot{m}_3.h_3 - \dot{m}_2.h_2$$

$$W = \dot{m}_2.h_2 - \dot{m}_1.h_1$$

The COP of the absorption system is defined as the heat load in the evaporator per heat load in the generator and work required for solution pump and it can be written as:

$$\mathbf{COP} = \frac{Q_{EVAP}}{Q_{GEN} + W_P}$$

Entropy Analysis :

$$\sum \dot{m}_{in} s_{in} = \sum \dot{m}_{out} s_{out}$$

Exergy Analysis :

The exergy is defined as the maximum probable reversible work that can be achieved by a system in transporting the state of the system with a location environment status[5]:

$$\psi = (h - h_0) - T_0(s - s_0)$$

The exergy destruction in each component can be written as:

$$\Delta\dot{\psi}_{EVAP} = \dot{m}_r(h_9 - T_0 s_9) - \dot{m}_r(h_{10} - T_0 s_{10}) + \dot{m}_{EVAP}((h_{17} - T_0 s_{17}) - (h_{18} - T_0 s_{18}))$$

$$\Delta\dot{\psi}_{COND} = \dot{m}_r(h_7 - T_0 s_7) - \dot{m}_r(h_8 - T_0 s_8) + \dot{m}_{COND}((h_{15} - T_0 s_{15}) - (h_{16} - T_0 s_{16}))$$

$$\Delta\dot{\psi}_{EDC} = \dot{m}_{ws}(h_2 - h_3 - T_0(s_2 - s_3) + \dot{m}_{ss}(h_4 - h_5 - T_0(s_4 - s_5)$$

$$\Delta\dot{\psi}_{GEN} = \dot{m}_{ws}(h_3 - T_0 s_3) - \dot{m}_{ss}(h_4 - T_0 s_4) - \dot{m}_r(h_7 - T_0 s_7) + \dot{m}_{GEN}((h_{11} - T_0 s_{11}) - (h_{12} - T_0 s_{12}))$$

$$\Delta\dot{\psi}_{ABS} = \dot{m}_{ss}(h_6 - T_0 s_6) - \dot{m}_{ws}(h_1 - T_0 s_1) + \dot{m}_r(h_{10} - T_0 s_{10}) + \dot{m}_{ABS}((h_{13} - T_0 s_{13}) - (h_{14} - T_0 s_{14}))$$

$$\Delta\dot{\psi}_P = \dot{m}_{ws}(h_1 - h_2 - T_0(s_1 - s_2)) + \dot{W}_p$$

$$\Delta\dot{\psi}_{VES} = \dot{m}_{ss}(h_5 - h_6 - T_0(s_5 - s_6))$$

$$\Delta\dot{\psi}_{VER} = \dot{m}_r(h_8 - h_9 - T_0(s_8 - s_9))$$

The total rate of exergy destruction of absorption system is the sum of exergy destruction in each component and can be written as[6]:

$$\Delta\dot{\psi}_{system}=\Delta\dot{\psi}_{GEN}+\Delta\dot{\psi}_{ABS}+\Delta\dot{\psi}_{COND}+\Delta\dot{\psi}_{EVAP}+\Delta\dot{\psi}_{EDC}+\Delta\dot{\psi}_{VES}+\Delta\dot{\psi}_{VER}+\Delta\dot{\psi}_{P}$$

the exergetic efficiency of the system is the ratio of the exergy produced in the evaporator to the exergy supplied to the generator. It can be written as[6]:

$$\eta_{exergetic}=\frac{\boldsymbol{Q_{EVAP}}\left|\left[\mathbf{1}-\frac{\boldsymbol{T_0}}{\boldsymbol{T_{EVAP}}}\right]\right|}{\boldsymbol{Q_{GEN}}\left[\mathbf{1}-\frac{\boldsymbol{T_0}}{\boldsymbol{T_{GEN}}}\right]+\boldsymbol{W_P}}$$

3.2. *Solar energy collecting system*

The rate of useful energy gain delivered by the solar collector can be defined as[7]:

$$\dot{\boldsymbol{Q}}_{\boldsymbol{u}}=\boldsymbol{A_C}*\boldsymbol{G}*\eta_{\boldsymbol{C}}$$

$\eta_{\boldsymbol{C}}$ the instantaneous collector efficiency (measure of the ηc collector performance) which is defined as the ratio of useful heat gain over the specified time

$$\eta_C=\boldsymbol{F_R}(\boldsymbol{\tau\alpha})-\boldsymbol{F_R U_L}\frac{\boldsymbol{T_m}-\boldsymbol{Ta}}{\boldsymbol{G}}$$

Perrin Brichambaut model

In 1975 Perrin Brichambaut proposed a model, which is a function of astronomical parameters. The above relationships are transformed into the following ones according to the atmospheric conditions.

The global solar radiation falling on the tilted collector surface is given by the following equation G (W/m^2)[8]:

$$\boldsymbol{G}=\boldsymbol{S}+\boldsymbol{D}$$

Where S and D are the direct and diffuse radiation

$S=A\cos\beta\,.\exp[\frac{-1}{B\sin(h+2)}]$

$D=\left(\frac{1+\cos i}{2}\right).D_H+\left(\frac{1-\cos i}{2}\right).Alb.G_H$

$D_H=A'(\sin h)^{0,4}$

$G_H=A''(\cos h)^{B''}$

where D_H : diffused irradiation received by a horizontal surface, G_H : overall irradiation received by a horizontal surface, alb : Soil Albedo (soil reflection coefficient).

Fundamental astronomy

Declination δ:

$$\delta=23{,}45\sin[\frac{360}{365}(n+284)]$$

Hour angle ω:

$$W=15°(TSV-15)$$

Sun’s Altitude :

The sun's altitude and azimuth angles can be determined in terms of the hour angle, declination angle, and latitude angle by the following formulas[8]:

$$\sin h = \sin\varphi \,.\, \sin\delta + \cos\varphi \,.\, \cos\delta \,.\, \cos w$$

$$\sin a = \frac{\cos\delta \,.\, \sin w}{\cos h}$$

A, B, A', A", B" are constants, that depend on the state of the atmosphere are presented in table 2.

State of the atmosphere	A	B	A'	A''	B''
Dark blue sky	1300	6	87	1150	1,14
Clear blue sky	1230	4	125	1080	1,22
Milky blue sky	1200	2,5	187	990	1,25

Table 2. *Parameters, describing the state of the atmosphere[8]*

4. Model validation

In order to validate the developed model, the results from this model have been compared with simulation data available from recent literature of Patel and Pandya. In the comparison, the values of input parameters (mainly the temperatures of the components and mass flow rate of the refrigerant) in the examined cases were identical. In the LiCl-H2O system, the parameters were as follows : (T_{GEN} = 78 °C ; T_{ABS} = 40 °C ;T_{COND}= 36 °C ; T_{EVAP} = 10 °C ; ε = 0,7 ; m_R = 0,00148 kg.s^{-1}).From this comparison it is observed that agreement between two model is satisfactory. The details are presented in Table 3 . It proves that the calculation model is valid and reliable.

	Symbol	Patel (kW)	Present study (kW)	Error (%)
Heat capacity of generator	Q_{GEN}	4,465	4,456	0,20
Heat capacity of evaporator	Q_{EVAP}	3,517	3,516	0,03
Heat capacity of absorber	Q_{ABS}	4,268	4,268	0
Heat capacity of condenser	Q_{COND}	3,705	3,705	0
Coefficient of performance	COP	0,7877	0,7891	0,17
Efficiency exergetic	$\eta_{exergetic}$	27,65%	27,7%	0,18

Table 3. *Comparison of present model with model of patel*

5. Simulation model

5.1. *Estimation of operating temperatures*

The searching ranges of temperatures specified for estimation of component temperatures (TE; TG; TC and TA) are as given below:

Range {T_{EVAP} : 1—10 °C;T_{GEN} : 50—90 °C;T_{COND} : 20—50 °C;T_{ABS} : 30—40 °C} . 9 combinations can be estimated are presented in table 4

	T_{EVAP} (°C)	T_{GEN} (°C)	T_{COND} (°C)	T_{ABS} (°C)	COP	Q_{EVAP} (kW)
1	2	78	39	35	0,46	0,389
2	3	72	34	35	0,632	0,8126
3	4	74	36	30	0,7819	3,587
4	5	68	33	35	0,7638	2 ,324
5	6	75	37	34	0,766	2,715
6	7	84	45	36	0,7531	3,162
7	8	70	32	37	0,7895	2,643
8	9	66	28	34	0,8364	4,762
9	10	78	36	40	0,7936	3,516

Table 4. *Estimated combinations of operating temperatures*

In this study, the software used for modelling is engineering equation solver (EES) [18]. The initial conditions used according to table 6 are the following: generator temperature as 66 °C, absorber temperature as 34 °C, condenser temperature as 28 °C, evaporator temperature as 9 °C and effectiveness of solution heat exchanger as 0,75 these parameters have to be determined from the table 6. System thermodynamic data and performance parameters are listed in Table 6 and 7 respectively. Based on these conditions, COP of system is calculated as 0.83. It is observed from Table 7 that under given operating condition, most of the exergy destruction occurred in generator and absorber. It is also found that exergy destruction in pump and expansion valve are very small and usually ignored.

	Temperature (°C)	X en (%)	Mass flow rate (kg/s)	Pression (kPa)	Enthalpy (kJ/kg)	Entropy (kJ/kg.K)
1	34	0,3861	0,05	1,148	136,3	0,3067
2	34	0,3861	0,05	3,782	136,3	0,3067
3	52,35	0,3861	0,05	3,782	186,1	0,464
4	66	0,4654	0,04148	3,782	275,1	0,5383
5	42	0,4654	0,04148	3,782	215,1	0,3549

6	44,28	0,4654	0,04148	1,148	215,1	0,3731
7	66	0	0,008524	3,782	2631	8,739
8	28	0	0,008524	3,782	117,3	0,4088
9	9	0	0,008524	1,148	117,3	0,4179
10	9	0	0,008524	1,148	2517	8,923
11	76	0	1,174	-	318,1	1,028
12	69	0	1,174	-	288,8	0,9427
13	26	0	1,127	-	108,9	0,381
14	31	0	1,127	-	129,9	0,4503
15	20	0	1,025	-	83,84	0,2962
16	25	0	1,025	-	104,8	0,367
17	16	0	0,9787	-	67,1	0,2387
18	11	0	0,9787	-	46,18	0,1657

Table 5. *Absorption system data obtained from the thermodynamic analysis*

Component	Energy (kW)	Exergy destruction (kW)	Non dimensional exergy loss (%)	COP
Generator	24,53	2,161	59,74 %	
Absorber	23,56	0,5676	15,75 %	
Evaporator	20,46	0,3381	9,38 %	
Condenser	21,43	0,4369	12,12 %	
Solution heat exchanger	2,487	0,07714	2,14 %	
Refrigerant expansion valve	-	0,02309	0,65 %	
Solution expansion valve	-	-	-	0,83
Pump	0,000005	0,000004	0,00001 %	
Total	92,47	3,604	100 %	

Table 6. *System's Performance parameters*

6. Results and discussions

6.1. *Variation of the coefficient of performance (COP) of the system according to the tepmerature: of evaporator (T_{EVAP}) and generature (T_{GEN})*

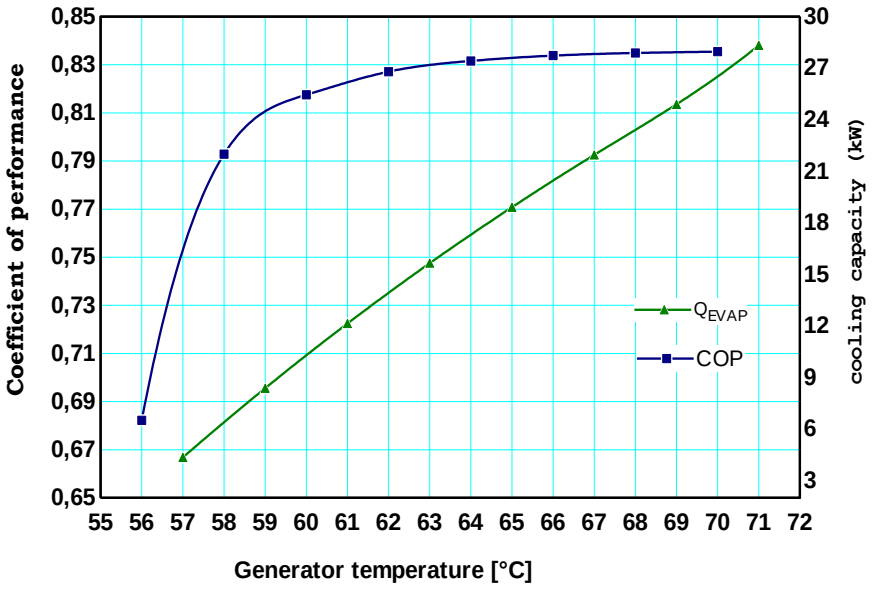

Figure 2. *Variation of the COP of the system according to the tepmerature: of generature (T_{GEN})*

Figures 2 present the variations of the coefficient of performance (COP) according to generator temperature. the COP and cooling capacity value increased sharply with generator temperature initially, but COP tended to level off. Moreover, a lower condensation and absorption temperature led to a greater COP.

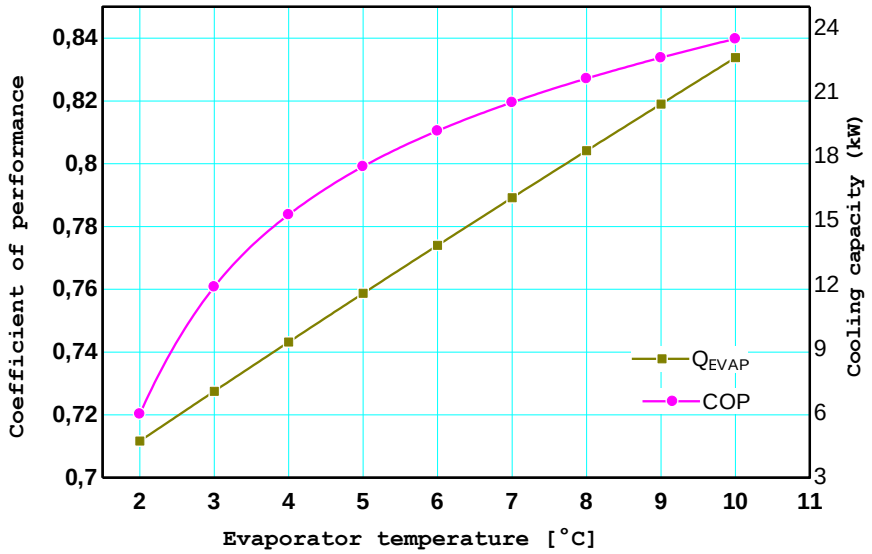

Figure 3. *Variation of the COP of the system according to the evaporator tepmerature (TEVAP)*

The variation of COP with evaporator temperature in the system is shown in Figure 3. It can be seen that the COP of system increased with evaporator temperature, and all the values approached 0.84 eventually. At this point, it is also important to state that a higher generator temperature was demanded to generate a lower evaporator temperature effect because the cooling production was harder to be achieved with low grade energy. Moreover, the COP was greater in the higher generator temperature at the same evaporator temperature level.

6.2. *Variation of the coefficient of performance (COP) of the system according to the temperatures of condenser (T_{COND}) and absorber (T_{ABS})*

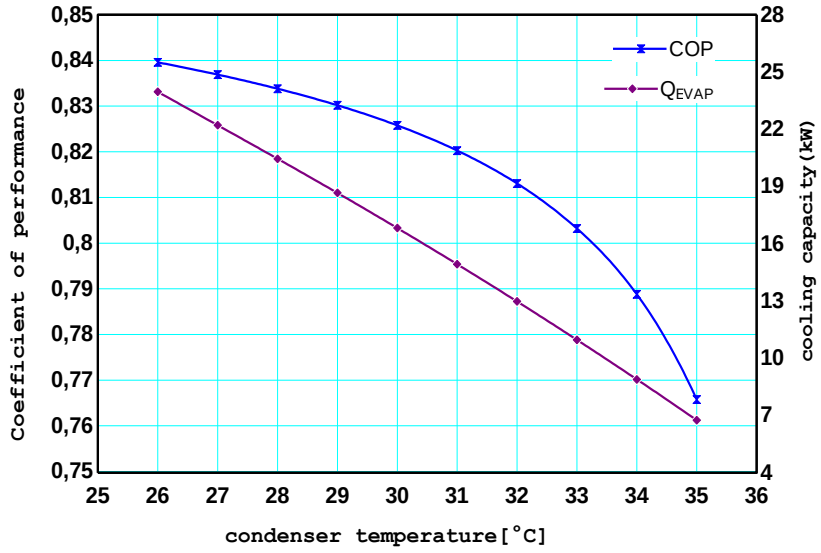

Figure 4. *Variation of the COP of the system according to the tepmerature of condenser (T_{COND})*

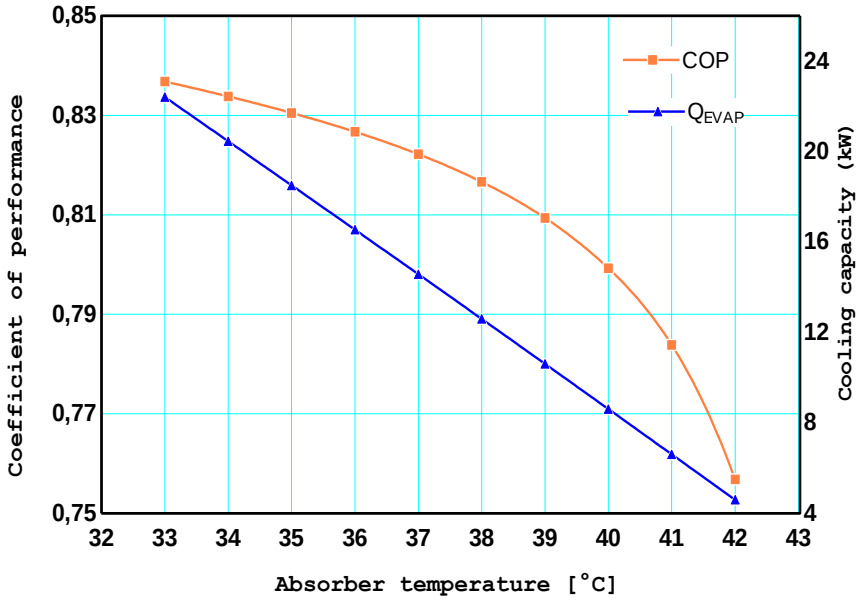

Figure 5. *Variation of the coefficient of performance (COP) of the system according to the temperature absorber (TABS)*

Figures 4 and 5 depict the effect of the condenser or absorber temperature on the COP. It can be seen that a decrease in COP occurred when the temperatures increases. Moreover, the performance of the system degraded more excessively in the high temperature zone.

If the condenser temperature was too small, the system operates some trouble because the concentration of strong solution got larger, which lead to the solution crystallization. On the other hand, the concentration of strong solution became lower with the increasing of the condenser temperature, which brought about the solution cycle ratio increase at a constant cooling capacity, and eventually resulted in the degradation of system performance for the heat load of a rapidly generator rising. There also the corresponding temperatures in LiCl-H2O system get higher.

6.3. *Variations of total exergy destruction and exergetic efficiency of the system according to the tepmeratures of condenser (T_{COND}) , evaporator (T_{EVAP}), generature (T_{GEN}) and absorber (T_{ABS}) :*

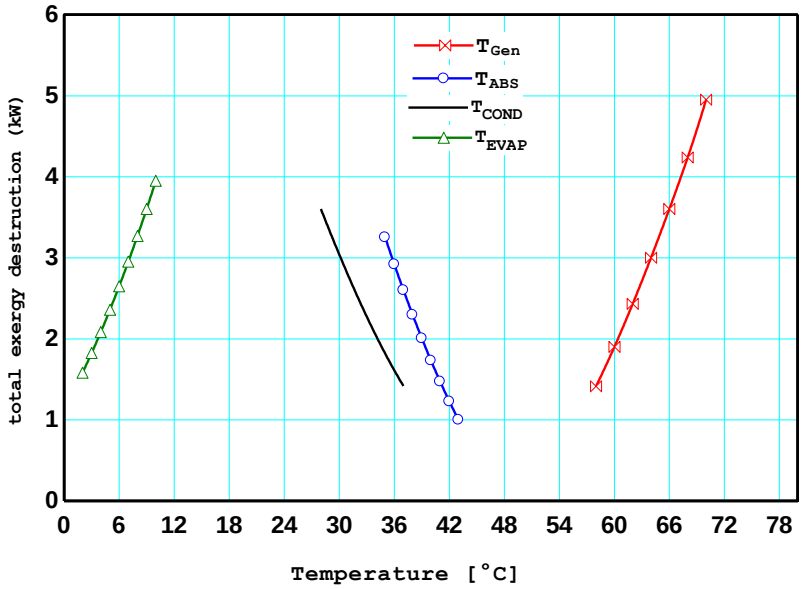

Figure 6. *Variations of total exergy destruction of the system according to the tepmeratures of condenser (T_{COND}) , evaporator (T_{EVAP}), generature (T_{GEN}) and absorber (T_{ABS})*

Figure 6 depict the effects of the evaporator, absorber, generator and condenser temperature on total exergy destruction of system. We note that total exergy destruction increases linearly with the increase of generator temperature. Moreover total exergy destruction decreases with the increased evaporator temperature under given operating condition.

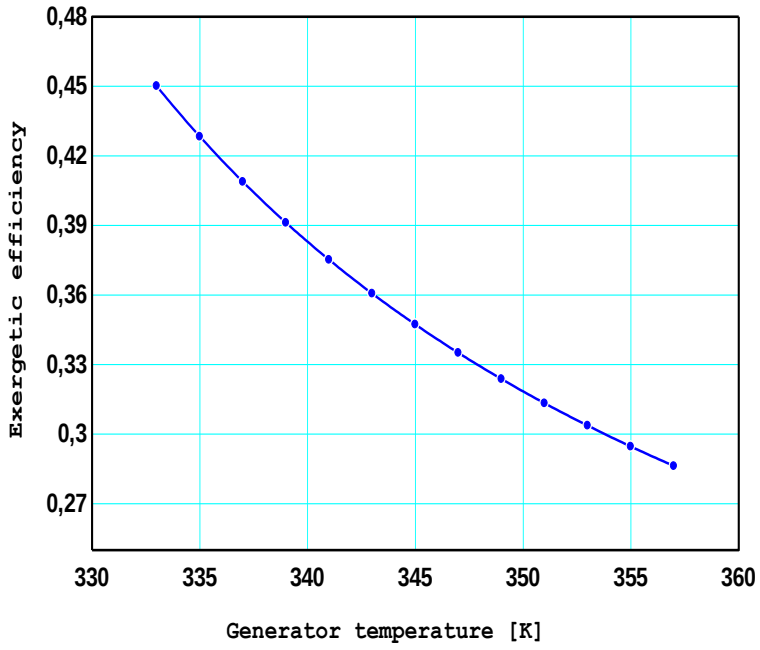

Figure 7. *Variations of exergetic efficiency of the system according to the tepmerature of generature (T_{GEN})*

It is found that exergetic efficiency of the system first increases with the decrease of generator temperature (Figures 7).

6.4. *Variations of total solar radiation*

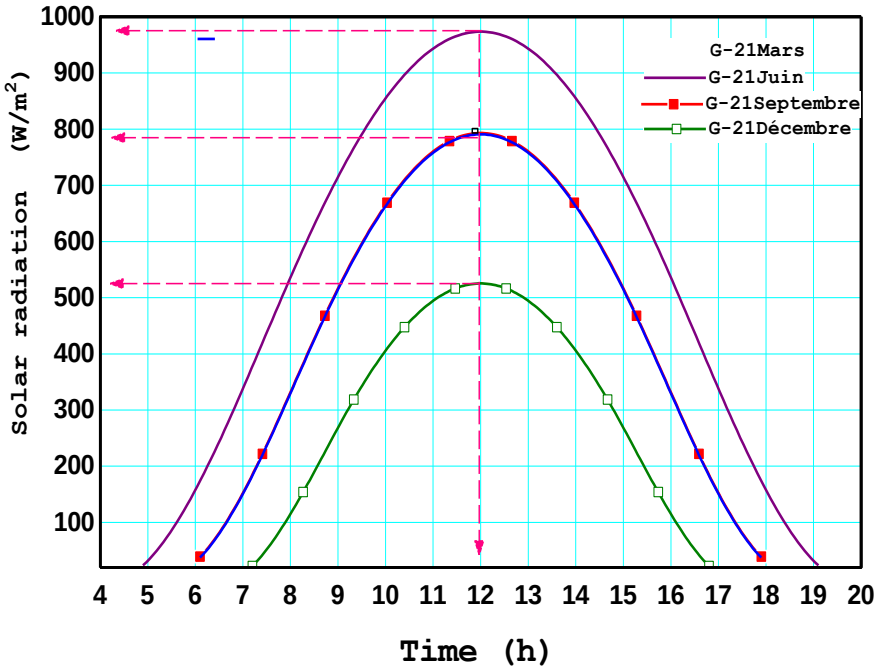

Figure 8. *Variations of total solar radiation*

The variations of total solar radiation are depicted in Figure 8. The global solar radiation of the winter solstice corresponding to December 21th, is between (0; 500 W/m^2), of the equinox corresponding to September 21th and March 21th have a radiation between (0; 780W/m^2) and of the summer solstice corresponding to June 21th is between (0; 980 W/m^2).we note that the radiation of June 21th is the most elevated.

6.5. *Variation of the collector efficiency*

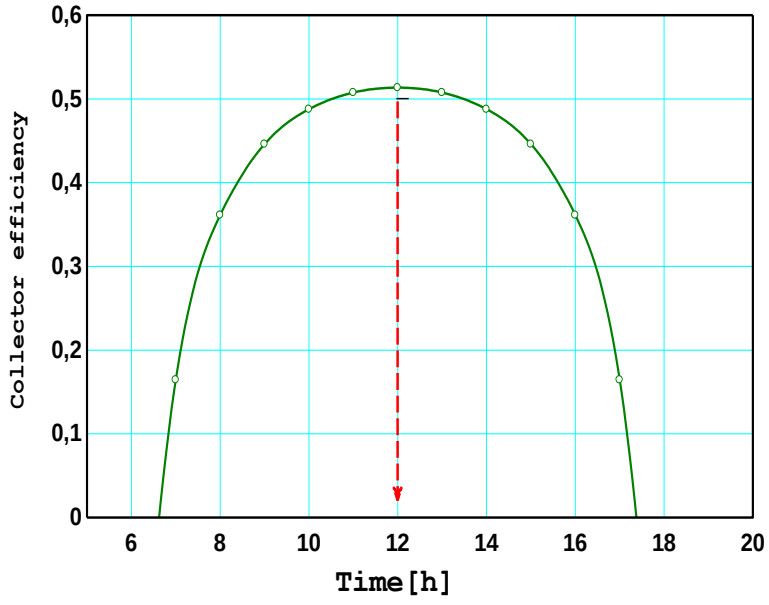

Figure 9. *The collector efficiency for a day in Gabes, Tunisia (Date: 21th June)*

It can be noticed from figure 9 that the collector efficiency varied significantly with the radiation intensity, reaching its highest value in the midday and falling sharply towards zero during the sunset. Using the weather input data (solar radiation and ambient temperature) of Gabes city in Tunisia for June 21th.

7. Conclusion

In this study, energy and exergy analysis of the solar-powered (H_2O-LiCl) absorption cooling system integrated with flat plate collector has been conducted. The following points can be concluded from this study:

- Increasing the generator temperature realize an increase of the COP. The cooling capacity is increased with the generator temperature while exergetic cooling is reduced. The rising of the generator inlet temperature also resulted in the increasing of the exergy loss through the components of the chiller system.
- Heat loads and exergy losses were less in the condenser and evaporator than those in the generator and absorber. This can be attributed to the irreversibilities associated with the heating and mixing of the solution (H_2O-LiCl) present in the generator and absorber, which was not found in the pure fluids through the condenser and evaporator
- The simulation shows that most of exergy destruction occurred in absorber and generator under given operating condition.
- Exergy destruction in pump and expansion valve is found to be the lowest.
- Using the weather input data (solar radiation and ambient temperature) of Gabes city for June 21, it can be noticed from figure 3 that the collector efficiency varied significantly with the radiation intensity, reaching its highest value in the midday and falling sharply towards zero during the sunset.

References

[1] R. Nikbakhti, X. Wang, A. K. Hussein, et A. Iranmanesh, « Absorption cooling systems – Review of various techniques for energy performance enhancement », *Alexandria Engineering Journal*, vol. 59, n° 2, p. 707-738, avr. 2020, doi: 10.1016/j.aej.2020.01.036.

[2] A. Aliane, S. Abboudi, C. Seladji, et B. Guendouz, « An illustrated review on solar absorption cooling experimental studies », *Renewable and Sustainable Energy Reviews*, vol. 65, p. 443-458, nov. 2016, doi: 10.1016/j.rser.2016.07.012.

[3] P. S. Arshi Banu et N. M. Sudharsan, « Review of water based vapour absorption cooling systems using thermodynamic analysis », *Renewable and Sustainable Energy Reviews*, vol. 82, p. 3750-3761, févr. 2018, doi: 10.1016/j.rser.2017.10.092.

[4] E. D. Kerme, A. Chafidz, O. P. Agboola, J. Orfi, A. H. Fakeeha, et A. S. Al-Fatesh, « Energetic and exergetic analysis of solar-powered lithium bromide-water absorption cooling system », *Journal of Cleaner Production*, vol. 151, p. 60-73, mai 2017, doi: 10.1016/j.jclepro.2017.03.060.

[5] T. K. Gogoi et D. Konwar, « Exergy analysis of a H2O–LiCl absorption refrigeration system with operating temperatures estimated through inverse analysis », *Energy Conversion and Management*, vol. 110, p. 436-447, 2016.

[6] J. Patel, B. Pandya, et A. Mudgal, « Exergy Based Analysis of LiCl-H 2 O Absorption Cooling System », *Energy Procedia*, vol. 109, p. 261-269, mars 2017, doi: 10.1016/j.egypro.2017.03.061.

[7] « Absorption cooling systems â€“ Review of various techniques for energy performance enhancement | Elsevier Enhanced Reader ».

[8] F. Chabane, F. Guellai, M. Y. Michraoui, D. Bensahal, A. Bima, et N. Moummi, « Prediction of the Global Solar Radiation on Inclined Area. Applied Solar Energy, 55 (1): 41-47 ». 2019.